Simultaneous Label-free and Pretreatment-free Detection of Heavy Metal Ions in Complex Samples Using Electrodes Decorated with Vertically-Ordered Silica Nanochannels

Bowen Cheng[1#], *Lin Zhou*[1#], *Lili Lu*[1], *Jiyang Liu*[1]*, *Xiaoping Dong*[1], *Fengna Xi*[1], *Peng Chen*[2]*

[1] Department of Chemistry, Zhejiang Sci-Tech University, 5 Second Avenue, Xiasha Higher Education Zone, Hangzhou, 310018, PR China

[2] Division of Bioengineering, School of Chemical & Biomedical Engineering, Nanyang Technological University, 70 Nanyang Drive, Singapore 637457

[#] These authors contributed equally to this work.

ABSTRACT: In this work, indium tin oxide coated glass (ITO) decorated with vertically-ordered mesoporous silica film (VMSF/ITO) is synthesized and applied as electrochemical sensor for simultaneous label-free and pretreatment-free detection of Pb^{2+}, Cu^{2+}, and Cd^{2+} in human serum and soil leaching solution. Using differential pulse voltammetry (DPV), the electrochemical detection consists of electro-deposition of metal species and subsequent anodic stripping in the silica nanochannels. Because of the electrostatic enrichment and nano-confinement effects, VMSF/ITO is able to simultaneously detect Pb^{2+}, Cu^{2+}, and Cd^{2+} in a mixture with low detection limits (2.6 nM, 32 nM and 230 nM, respectively). Moreover, VMSF confer the electrode with excellent anti-fouling and anti-interference property through steric exclusion and electrostatic repulsion. Direct analysis of complex biological (human serum) and environmental (soil leaching solution) samples could be finished within 10 min without the usual need of tedious pretreatment. Furthermore, the VMSF/ITO sensor can be reused for several times without performance degradation.

KEYWORDS: electrochemical sensing; vertically-ordered silica nanochannels; detection of heavy metal ions

Introduction

With ever-increasing industrialization, heavy metal ion species have become common contaminants in water, soil and food. Due to the non-biodegradability, toxic heavy metal ions impose a great threat to living organisms [1-4]. For instance, even at a trace concentration, lead(II) (Pb^{2+}, 10 ng/mL) could cause fearful damage to brain, immune system, liver, kidney, and central nervous system especially to young people and children [5-7]. And a small amount of cadmium(II) (Cd^{2+}) may cause renal dysfunction, metabolism disorders, and increase cancer incidence [8,9]. Though appropriate quantity of copper(II) (Cu^{2+}) is nutrient as the co-factor of some enzymes, elevated concentrations of Cu^{2+} may lead to gastrointestinal disturbance and liver or kidney damage [10-12]. Hence, realizing simple, sensitive and simultaneous detection of heavy metal ion species are of great importance. Comparing to other techniques including flam or graphite furnace atomic absorption spectrophotometry (FAAS/GFAAS), inductively-coupled plasma mass spectrometry (ICP-MS) and fluorescence detection, electrochemical sensing is particularly attractive because of high sensitivity, rapid analysis, no need of bulky instrumentation and easy operation [2,13-16]. Current electrochemical sensors, however, are often unpractical for analysis of complex clinical (e.g. serum or whole blood) or environmental (e.g., soil leaching solution, waste water) samples due to unsatisfactory selectivity, stability and reproducibility, because of interference from other redox molecules and non-specific fouling on the sensor surface [17,18]. Various strategies have been developed to improve the anti-fouling and anti-interference characteristics of electrochemical sensors. Commonly, molecular passivation layers are coated on the sensor surface, which reduce non-specific interactions by introducing electrostatic repulsion (e.g., perfluorinated ionomer Nafion or other polyelectrolyte [19-21]) or steric hindrances (e.g., spatial spacers of alkyl chains with certain lengths or polymer brushes [22,23]). However, the detection efficiency is unavoidably compromised to some extent due to

obstruction of diffusion and charge transfer.

Recently, vertically-ordered mesoporous silica film (VMSF) has attracted tremendous interests as the selectivity layer for electrochemical sensors [17,24-32]. VMSF exhibits uniform nanochannels (2-3 nm) perpendicular to the underlying electrode with a high pore density (~40000 μm^{-2}). Such unique nanostructure is advantageous [33-40] in term of (1) anti-fouling and anti-interface effects because non-specific adsorption of macromolecules onto the electrode could be remarkably eliminated via steric hinderance; (2) anti-interference ability due to repulsion of negatively charged redox compounds (e.g. ascorbic acid, uric acid) by the negatively charged deprotonated silanol groups on the channel surface; (3) improved sensitivity towards positively charged analytes resulting from the enrichment effect enabled by electrostatic attraction and spatial confinement inside the channel; (4) fast detection due to unhindered molecular transport inside the channel.

In this work, simultaneous label-free and pretreatment-free detection of heavy metal ion species in complex biological and environmental samples is presented using ITO electrodes decorated with vertically-ordered mesoporous silica nanochannels (VMSF). The detection is based on metal ion enrichment through electrostatic and coordination effects by negatively charged VMSF nanochannels, subsequent electrochemical deposition and anodic stripping (Fig. 1). The VMSF/ITO sensor demonstrated outstanding performance for simultaneous analysis of Pb^{2+}, Cu^{2+} and Cd^{2+} in human serum and soil leaching solution in terms of excellent anti-interference and anti-fouling property, fast detection, high sensitivity and selectivity, and good reusability.

Material and methods

2.1. Reagents and apparatus

Standard Pb^{2+}, Cu^{2+} and Cd^{2+} solutions were obtained from National standard materials center (China). Tetraethyl orthosilicate (TEOS), cetyltrimethylammonium bromide (CTAB), potassium ferricyanide ($K_3Fe(CN)_6$), potassium hydrogen phthalate (KHP), ammonia aqueous solution (wt. 25%), sodium acetate (NaAc), acetic acid (HAc) and high-purity HNO_3 were obtained from Aladdin Chemistry Co. Ltd. (China).

ITO coated glass (ITO thickness: ~100 nm, resistance: <14.5 Ω/square) was obtained from Zhuhai Kaivo Electronic components (Zhuhai, China). All aqueous solutions were prepared with ultrapure water (18.2 MΩ cm, Milli-Q, Millipore).

2.2. Materials characterizations

Scanning electron microscopy (SEM) was conducted on a field-emission scanning electron microscopy (S-4800, Hitachi, Japan). Transmission electron microscopic (TEM) photograph was taken on a JEM-2100 transmission electron microscope (JEOL Ltd., Japan) at operating voltage of 200 kV. Vertically-ordered mesoporous silica film (VMSF) was mechanically scrapped from the surface of ITO electrodes, dispersed in ethanol by sonication and dropped onto the copper grid. Zeta potential for solid phase was recorded on Surpass zeta potential system (Anton parr, Austria). Electrochemical experiments were carried out on an Autolab PGSTAT302N electrochemical workstation (Metrohm, Switzerland). A three electrodes system was adopt with bare or modified ITO as working electrode, Ag/AgCl (saturated KCl solution) as reference electrode and Pt-sheet electrode as counter electrode. Graphite furnace atomic absorption spectroscopy 900T (GFAAS, PE, USA) were used to measure Pb^{2+}, Cu^{2+} and Cd^{2+} as the current golden standard.

2.3. Preparation of VMSF/ITO electrode

ITO electrode was used as the supporting electrode. It was firstly immersed in 1 M NaOH overnight followed with successive clean by acetone, ethanol and ultrapure water under ultrasonication. VMSF was then fabricated on ITO electrode using Stöber-solution growth approach as previously reported [41]. Briefly, TEOS hydrolyzes and assembles in presence of CTAB surfactant micelles (SM) in ammonia-ethanol medium. After removal of SM by solvent extraction in 0.1 M HCl of ethanol solution, VMSF/ITO sensor was obtained.

2.4 Simultaneous electrochemical detection of Pb^{2+}, Cu^{2+} and Cd^{2+}

NaAc-HAc buffer (0.1 M, pH 5.0) was used as the medium for metal detection. Standard stock solutions of Pb^{2+} and Cu^{2+} and Cd^{2+} (50.0 mM) were prepared and further diluted stepwise to obtain different concentrations. Electrochemical detection of metal ions consists of electrochemical deposition and the following stripping.

Firstly, metal species were deposited on VMSF/ITO at -0.90 V for 300 s by reduction of Pb^{2+}, Cu^{2+} and Cd^{2+}. Secondly, anodic stripping (-0.95 to 0.4 V) of the electrodeposited Cd, Pb and Cu was detected using differential pulse voltammetry (DPV, modulation amplitude: 0.05 V, modulation time: 0.05 s, interval time: 0.4 s).

Human blood serum (healthy man) and soil leaching solution (SLS, soil from uncontained vegetable field, 2g soil/10 mL solution, pH 5.5) were provided by Center for Disease Control and Prevention (Hangzhou, China) for real sample analysis. The electrochemical measurement was directly performed by dilution SLS using buffer (v/v = 1:1) for pH adjustment. For serum, protein-bound Pb^{2+} and Cu^{2+} ions are firstly released (WS/T 174-1999, WS/T 93-1996, China). Briefly, serum (2 mL) was mixed with diluted nitric acid (0.7 M, 4 mL) and stirred for 1 min. After pH was adjusted to 5.0 using NaOH (2 M), the final volume of the solution was modified to 10 mL using buffer solution for further electrochemical analysis. The reliability of electrochemical detection was also evaluated using standard addition method. A defined amount of ions was added into original serum or soil leaching solution. The obtained samples with artificial concentrations were also determined using the same procedure as described above. For measurement using standard GFAAS, samples were treated using the same methods and the supernatants after high speed centrifugation are analyzed.

3. Results and discussion

3.1. Preparation and characterization of VMSF/ITO electrodes

As previously reported [41] and illustrated in Fig. 1, vertically-ordered mesoporous silica film (VMSF) was readily prepared on ITO electrode using Stöber-solution growth where the silica precursor, tetraethyl orthosilicate (TEOS), hydrolyzes and assembles in the presence of cetyltrimethylammonium bromide (CTAB) surfactant micelles (SM) in ammonia-ethanol medium. CTAB micelles were then easily removed by solvent extraction in HCl-ethanol solution [29-33]. As shown in Fig. 2A and B, the cross-section SEM images of SM@VMSF/ITO and VMSF/ITO exhibit three layers from top to bottom corresponding to SM@VMSF or VMSF, ITO and glass, respectively. Fig. 2C and D display the high-resolution TEM (HRTEM)

images of SM@VMSF and VMSF scraped from the ITO surface. As seen, both films are continuous and uniform with mesopores (~2.6 nm) homogeneously distributed over the entire film. After removal of SM, no obvious changes in morphology or thickness were observed, indicating the stability of the VMSF. Although the structure of SiO_2 is easy to collapse under high-energy electron beams, some vertical channels can still be seen from the cross-section TEM image of VMSF (Fig. S1).

The permeability of silica nanochannel modified electrode was investigated by cyclic voltammetry measurement of the standard redox probes. Before removal of CTAB micelles, almost no redox responses are produced by positively charged $Ru(NH_3)_6^{3+}$ probe (Fig. S2A) or negatively charged $Fe(CN)_6^{3-}$ probe (Fig. S2B), suggesting that CTAB micelles block the access of charged redox probes. After removal of CTAB micelles, the redox peaks for both probes are observed in VMSF/ITO, indicating the opening of nanochannels. Compared with bare ITO electrode, VMSF/ITO gives significantly increased peak current for $Ru(NH_3)_6^{3+}$ (Fig. S2A) and decreased electrochemical signal for $Fe(CN)_6^{3-}$, indicating the electrostatic enrichment of positively charged molecules in the nanochannels [41] due to the negative charges (Fig. S3) from the deprotonated surface silanols (pKa of ~2 [42]).

3.2. Optimal conditions for metal ion detection

In view of the ability of VMSF nanochannels to electrostatically enrich positively-charged ultra-small analytes while excluding interferences by size- and/or charge-screening, VMSF/ITO is particularly ideal for detection of metal ions. The electrochemical detection used here consists of the electro-deposition of M^{2+} (M = Cd, Pb and Cu) and the following anodic stripping (Fig. 1) realized by differential pulse voltammetry (DPV). In order to achieve high sensitivity for simultaneous determination of Pb^{2+}, Cu^{2+} and Cd^{2+}, the experimental conditions including deposition potentials, pH value and deposition time were optimized. To ensure sufficient reduction of heavy metal ion, the deposition potential needs to be more negative compared with the stripping potential. To cope with the striping potentials (Cd^{2+}, Pb^{2+} and Cu^{2+} at about -0.8 V, -0.5 V and -0.1 V vs Ag/AgCl, respectively) and the negative potential window of ITO (~-1.2 V), the deposition potential is finally set

as -0.9 V to ensure simultaneous and fast deposition of all three ion species. As illustrated in Fig. 3A, the pH value in deposition process affects the stripping signal of each ion. The low pH values (from 2.0 to 3.0) result in an obvious decrease of signal due to protonation of silica hydroxyl which weakens absorption and coordination of metal ions on the nanochannel surface. On the other hand, the currents at high pH values (e.g., pH 6.0) also reduce due to possible formation of metal hydroxide complexes. To avoid the hydroxylation of metal ions, the optimal pH value for simultaneous detection is determined as 5.0. A series of accumulation times from 10 to 600 s were investigated. As shown in Fig. 3B, the stripping signal sharply increases while deposition time increases, suggesting the improved accumulation of metal species in VMSF nanochannels. But stripping signal reaches a plateau as the deposition time goes beyond 300 s, presumably because the active sites on VMSF/ITO electrode are saturated by metal ion interaction. Therefore, the optimal electrodeposition time is set at 300 s. The facilitating roles of VMSF nanochannels and electrochemical electrodeposition in enhancing the detection signal via promoting accumulation of metal species are evidenced by the observations that i) the stripping signals of three metal ions on ITO/VMSF are larger than those obtained from bare ITO electrode; ii) when electrodeposition is not applied, very small stripping signals are produced (Fig. S4).

3.3. Individual and simultaneous detection of Pb^{2+}, Cu^{2+} and Cd^{2+} using VMSF/ITO

Fig. 4A-C show that the stripping peaks towards, Cu^{2+}, Pb^{2+}, Cd^{2+} and appear at -0.1 V, -0.50V, -0.83V, respectively. Separation of the striping potentials promises simultaneous detection of multiple ion species. The stripping peak current of each ion type increases with increasing ion concentration. Good linear correlation is found between the stripping current and the centration from 25.0 nM to 50.0 μM for Pb^{2+}, 100.0 nM to 40.0 μM for Cu^{2+}, 1.0 μ M to 20.0 μM for Cd^{2+}. The limits of detection (LOD) of Pb^{2+}, Cu^{2+} and Cd^{2+} ions are determined as low as 2.4 nM, 20 nM and 140 nM respectively at a signal-to-noise ratio of 3. Due to the relative lower coordination affinity between Cd^{2+} and SiO_2 [43], Cd^{2+} exhibits the highest LOD and the narrowest linear range among the three ion species. Detection of one ion type with varying

concentrations in the presence of a fixed concentration of the other two ion types (10 μM) are demonstrated in Fig. 4D-F. The VMSF/ITO sensor is able to detect Pb^{2+} (25.0 nM ~ 40.0 μM), Cu^{2+} (100.0 nM ~ 30.0 μM) and Cd^{2+} (1.0 μM ~ 20.0μM) with LOD of 2.6 nM, 32 nM and 230 nM, respectively. Comparing to the individual analysis, the liner range and sensitivity for the detection of Cu^{2+} and Pd^{2+} remain unchanged. However, reduction in sensitivity is observed for Cd^{2+}. This may be caused by the formation of Cu-Cd and Pb-Cd alloys when Cd, Cu and Pb co-electrodeposited on electrode surface. As Cd is the first to dissolve in the potential scanning process, the formation of metallic alloys decreased its stripping current [44,45].

Comparison between electrochemical detection of Cu^{2+}, Pb^{2+} and Cd^{2+} using differently modified electrode is provided in Table S1. The LOD for each ion is lower than those obtained using Au nanoparticles (AuNPs) [46], nanoplate-stacked Fe_3O_4 modified GCE [47] modified glassy carbon electrode (GCE) and magnetite-decorated oxidized ordered mesoporous carbon (OMC-OXI-Fe) modified graphite electrode [48]. The LOD for Pb^{2+} is also lower than graphene oxide doped diaminoterthiophene/Nafion-modified screen-printed carbon electrode (GO/DTT/Nafion-modified SPCE) [49], 4-carboxybenzo-18-crown-6 modified graphite electrodes [50], metal-organic frameworks (MIL-100(Cr)) [51] or nafion-hydroxyapatite [52], christmas tree-like cerium hexacyanoferrate (CeHCF) [53] or reduced GO supported spongy AuNPs (rGO@AuNPs) [54] modified GCE. The detected concentration of Cu^{2+} is lower than that of $-NH_2$ modified [33] and Cu(II)-specific DNAzyme-functionalized [55] VMSF/Au elctrode.

The anti-interference characteristic is vital for practical application of electrochemical sensors. Simultaneous detection of Pb^{2+}, Cu^{2+} and Cd^{2+} was examined in presence of some possible interfering species including biologically relevant species including glucose (Glu), dopamine (DA), horseradish peroxidase (HRP), starch, hemoglobin (Hb) and commonly co-existed Fe^{3+} and Ni^{2+} ions. Fig. 5A displays the relative signal changes (I/I_0) calculated using the stripping currents in the absence (I_0) or presence (I) of interfering substrate. Even large dose of each

interference (600.0 mg/L) is added into the solution containing Cd^{2+} (10 μM, 1.1 mg/L), Pb^{2+} (10 μM, 2.1 mg/L), and Cu^{2+} (10 μM, 0.6 mg/L), no obvious change of peak currents for each ion was noticed (Fig. 5A).

The relative standard deviation (RSD) for detection of Pb^{2+}, Cu^{2+} or Cd^{2+} from five independently prepared electrodes is within 4.0%. Additionally, the detection signal remains >91% of its initial response after being reused for 10 times (Fig. 5B). In addition to the excellent reproducibility and reusability, the cost of VMSF/ITO electrode (0.5 × 5 cm) is estimated to be < $ 1, promising for cheap, disposable and reliable use.

3.4. Analysis of complex environmental and biological samples

The application of VMSF/ITO sensor for simultaneous detection of Pb^{2+}, Cu^{2+} and Cd^{2+} in environmental samples (soil leaching solution，SLS) and biological sample (human serum) is demonstrated (Table 1). Conventional electrochemical sensors are hardly able to directly analyze complex samples unless there is a pretreatment process (e.g. selective precipitation, centrifugation, filtration, dialysis, etc.) because of serious fouling of sensor surface and interference from other redox compounds. Here, ions originally existed or spiked into the serum sample and soil leaching solution (photograph shown in Fig. S5) can be directly and faithfully detected (only pH adjustment is needed). Fig. 6 gives the comparison of DPV stripping signals on VMSF/ITO and ITO electrodes for detection of Cu^{2+} and Pb^{2+} in serum or SLS. ITO electrode exhibits poor signals for serum analysis presumably because of electrode fouling caused by absorbed proteins from serum. Similarly, due to the fouling from the absorbed particulates and interference from large organic compounds in soil leaching solution, ITO also exhibits low and distorted signals (Fig. 6B). The results suggest that VMSF nanochannels act not only as signal enhancer as discussed above but also good anti-fouling barrier. As shown, the obtained results are in good agreement with that from the current golden standard i.e. graphite furnace atomic absorption spectroscopy (GFAAS) method. Using both our method and GFAAS, Cd^{2+} is not detectable in healthy human serum (<45 nM [56]) and uncontaminated soil (< 0.4 μmol/L; 2g soil in 10 ml SLS, GB15618-2008, China).

The recovery determined by adding a known amount of ions is satisfactory (between 97.8% to 104.8%). Our method is sensitive enough to detect the tolerance level of Pb^{2+} and Cu^{2+} in human serum (Pb^{2+} < 0.48 μM, Cu^{2+}: 12 ~ 25 μM [57]) or in soil (Pb^{2+} < 0.5 μM, Cu^{2+} < 1.6 μM; $m_{soil\ (g)}/V_{extraction\ solution\ (ml)}$ = 1:5, GB15618-2008, China). It is also worth-noting that each analysis can be finished within 10 min because no sophisticated pre-treatments are needed. In comparison with GFAAS which requires expensive instrument, special skills and high energy consumption, the present electrochemical method is simple, convenient, fast, and of low-cost, which is particularly suitable for on-site detection.

4. Conclusion

The VMSF/ITO electrode has been employed for simultaneous electrochemical detection of heavy metal ion species in environmental and clinical samples. The sensor is highly sensitive because of the electrostatic enrichment and nano-confinement effects. The VMSF nanochannles confer the electrode with excellent anti-fouling and anti-interference property through steric exclusion and electrostatic repulsion. Consequently, the sensor can be used to directly analyze complex samples without the usual need of tedious pretreatment; and the sensor can be reused for several times without performance degradation.

Acknowledgements

We gratefully acknowledge valuable discussions with Prof. Bin Su and Dr. Fei Yan (Zhejiang Univ., China) for the preparation of VMSF. We acknowledge the financial support from the financial support from the National Natural Science Foundation of China (No. 21305127), the Zhejiang Provincial Natural Science Foundation of China (LY15B050006，LY17B050007), and 521 talent project of ZSTU.

References

[1] L. Ma, Q. Wang, S.M. Islam, Y. Liu, S. Ma, M.G. Kanatzidis, Highly selective and efficient removal of heavy metals by layered double hydroxide intercalated with the MoS_4^{2-} Ion, J. Am. Chem. Soc. 138 (2016) 2858-2866.

[2] Renu, M. Agarwal, K. Singh, Heavy metal removal from wastewater using various adsorbents: a review, J. Water Reuse Desalin. 7 (2017) 387-419.

[3] B. Bansod, T. Kumar, R. Thakur, S. Rana, I. Singh, A review on various electrochemical techniques for heavy metal ions detection with different sensing platforms, Biosens. Bioelectron. 94 (2017) 443-455.

[4] W.Y. Zhou, J.Y. Liu, J.Y. Song, J.J. Li, J.H. Liu, X.J. Huang, Surface-electronic-state-modulated, single-crystalline (001) TiO_2 nanosheets for sensitive electrochemical sensing of heavy-metal ions, Anal. Chem. 89 (2017) 3386-3394.

[5] K. Huang, B. Li, F. Zhou, S. Mei, Y. Zhou, T. Jing, Selective solid-phase extraction of lead ions in water samples using three-dimensional ion-imprinted polymers, Anal. Chem. 88 (2016) 6820-6826.

[6] S. Bian, C. Shen, H. Hua, L. Zhou, H. Zhu, F. Xi, J. Liu, X. Dong, One-pot synthesis of sulfur-doped graphene quantum dots as a novel fluorescent probe for highly selective and sensitive detection of lead(II), RSC Adv. 6 (2016) 69977-69983.

[7] B. Zhang, J. Chen, H. Zhu, T. Yang, M. Zou, M. Zhang, M. Du, Facile and green fabrication of size-controlled AuNPs/CNFs hybrids for the highly sensitive simultaneous detection of heavy metal ions, Electrochim. Acta 196 (2016) 422-430.

[8] D. Martin-Yerga, I. Alvarez-Martos, M. Carmen Blanco-Lopez, C.S. Henry, M. Teresa fernandez-abedul, Point-of-need simultaneous electrochemical detection of lead and cadmium using low-cost stencil-printed transparency electrodes, Anal. Chim. Acta 981 (2017) 24-33.

[9] D. Jedryczko, P. Pohl, M. Welna, Determination of the total cadmium, copper, lead and zinc concentrations and their labile species fraction in apple beverages by flow-through anodic stripping chronopotentiometry, Food Chem. 225 (2017) 220-229.

[10] C. Shen, S. Ge, Y. Pang, F. Xi, J. Liu, X. Dong, P. Chen, Facile and scalable preparation of highly luminescent N,S co-doped graphene quantum dots and

their application for parallel detection of multiple metal ions, J. Mater. Chem. B 5 (2017) 6593-6600.

[11] S. Lee, G. Barin, C.M. Ackerman, A. Muchenditsi, J. Xu, J.A. Reimer, S. Lutsenko, J.R. Long, C.J. Chang, Copper capture in a thioether-functionalized porous polymer applied to the detection of wilson's disease, J. Am. Chem. Soc. 138 (2016) 7603-7609.

[12] Y. Yang, A.A. Ibrahim, P. Hashemi, J.L. Stockdill, Real-time selective detection of copper(II) using ionophore-grafted carbon-fiber microelectrodes, Anal. Chem. 88 (2016) 6962-6966.

[13] P.S. Pakchin, S.A. Nakhjavani, R. Saber, H. Ghanbari, Y. Omidi, Recent advances in simultaneous electrochemical multi-analyte sensing platforms, TrAC, Trends Anal. Chem. 92 (2017) 32-41.

[14] F. Xi, D. Zhao, X. Wang, P. Chen, Non-enzymatic detection of hydrogen peroxide using a functionalized three-dimensional graphene electrode, Electrochem. Commun. 26 (2013) 81-84.

[15] Z. Zhang, H. Ji, Y. Song, S. Zhang, M. Wang, C. Jia, J.Y. Tian, L. He, X. Zhang, C.S. Liu, Fe(III)-based metal-organic framework-derived core-shell nanostructure: sensitive electrochemical platform for high trace determination of heavy metal ions, Biosens. Bioelectron. 94 (2017) 358-364.

[16] Q. Sun, J. Wang, M. Tang, L. Huang, Z. Zhang, C. Liu, X. Lu, K.W. Hunter, G. Chen, A new electrochemical system based on a flow-field shaped solid electrode and 3D-printed thin-layer flow cell: detection of Pb^{2+} ions by continuous flow accumulation square-wave anodic stripping voltammetry, Anal. Chem. 89 (2017) 5024-5029.

[17] F. Yan, X. Lin, B. Su, Vertically ordered silica mesochannel films: electrochemistry and analytical applications, Analyst 141 (2016) 3482-3495.

[18] F. Yan, W. Zheng, L. Yao, B. Su, Direct electrochemical analysis in complex samples using ITO electrodes modified with permselective membranes consisting of vertically ordered silica mesochannels and micelles, Chem. Commun. 51 (2015) 17736-17739.

[19] X. Pang, P. Imin, I. Zhitomirsky, A. Adronov, Conjugated polyelectrolyte complexes with single-walled carbon nanotubes for amperometric detection of glucose with inherent anti-interference properties, J. Mater. Chem. 22 (2012) 9147-9154.

[20] X. Yang, F.B. Xiao, H.W. Lin, F. Wu, D.Z. Chen, Z.Y. Wu, A novel H_2O_2 biosensor based on Fe_3O_4-Au magnetic nanoparticles coated horseradish peroxidase and graphene sheets-Nafion film modified screen-printed carbon electrode, Electrochim. Acta 109 (2013) 750-755.

[21] G.M.P. Morrison, M. Florence, Electrochemical speciation analysis of metals at membrane-coated electrodes, Electroanalysis 1 (1989) 485-491.

[22] A. Miodek, E.M. Regan, N. Bhalla, N.A.E. Hopkins, S.A. Goodchild, P. Estrela, Optimisation and characterisation of anti-fouling ternary SAM layers for impedance-based aptasensors, Sensors 15 (2015) 25015-25032.

[23] W. Zhao, Q. Ye, H. Hu, X. Wang, F. Zhou, Grafting zwitterionic polymer brushes via electrochemical surface-initiated atomic-transfer radical polymerization for anti-fouling applications, J. Mater. Chem. B 2 (2014) 5352-5357.

[24] A. Walcarius, Mesoporous materials and electrochemistry, Chem. Soc. Rev. 42 (2013) 4098-4140.

[25] N. Vila, J. Ghanbaja, E. Aubert, A. Walcarius, Electrochemically assisted generation of highly ordered azide-functionalized mesoporous silica for oriented hybrid films, Angew. Chem., Int. Ed. 53 (2014) 2945-2950.

[26] W. Li, L. Ding, Q. Wang, B. Su, Differential pulse voltammetry detection of dopamine and ascorbic acid by permselective silica mesochannels vertically attached to the electrode surface, Analyst 139 (2014) 3926-3931.

[27] N. Vila, J. Ghanbaja, A. Walcarius, Clickable bifunctional and vertically aligned mesoporous silica films, Adv. Mater. Interfaces 3 (2016) 1500440.

[28] X. Lin, Q. Yang, L. Ding, B. Su, Ultrathin silica membranes with highly ordered and perpendicular nanochannels for precise and fast molecular deparation, ACS Nano 9 (2015) 11266-11277.

[29] I. Cesarino, E.T.G. Cavalheiro, C.M.A. Brettb, Simultaneous determination of

cadmium, lead, copper and mercury ions using organofunctionalized SBA-15 nanostructured silica modified graphite–polyurethane composite electrode, Electroanalysis 22 (2010) 61-68.

[30] W. Yantasee, Y.H. Lin, T.S. Zemanian, G.E. Fryxell, Voltammetric detection of lead(II) and mercury(II) using a carbon paste electrode modified with thiol self-assembled monolayer on mesoporous silica (SAMMS), Analyst 128 (2003) 467-472.

[31] G. Herzog, N.A. Vodolazkaya, A. Walcarius, Platinum ultramicroelectrodes modified with electrogenerated surfactant-templated mesoporous organosilica films: effect of film formation conditions on its performance in preconcentration electroanalysis, Electroanalysis 25 (2013) 2595-2603.

[32] G. Herzog, E. Sibottier, M. Etienne, A. Walcarius, Electrochemically assisted self-assembly of ordered and functionalized mesoporous silica films: impact of the electrode geometry and size on film formation and properties, Faraday Discuss. 164 (2013) 259-273.

[33] M. Etienne, A. Goux, E. Sibottier, A. Walcarius, Oriented mesoporous organosilica films on electrode: A new class of nanomaterials for sensing, J. Nanosci. Nanotechnol. 9 (2009) 2398-2406.

[34] W. Liu, X. Yan, J. Lang, Q. Xue, Electrochemical behavior of graphene nanosheets in alkylimidazolium tetrafluoroborate ionic liquid electrolytes: influences of organic solvents and the alkyl chains, J. Mater. Chem. 21 (2011) 13205-13212.

[35] J. Liu, D. He, Q. Liu, X. He, K. Wang, X. Yang, J. Shangguan, J. Tang, Y. Mao, Vertically ordered mesoporous dilica film-assisted label-free and universal electrochemiluminescence aptasensor platform, Anal. Chem. 88 (2016) 11707-11713.

[36] M.S. Wu, X.T. Sun, M.J. Zhu, H.Y. Chen, J.J. Xu, Mesoporous silica film-assisted amplified electrochemiluminescence for cancer cell detection, Chem. Commun. 51 (2015) 14072-14075.

[37] Q. Sun, F. Yan, L. Yao, B. Su, Anti-biofouling isoporous silica-micelle membrane

enabling drug detection in human whole blood, Anal. Chem. 88 (2016) 8364-8368.

[38] Q. Yang, X. Lin, B. Su, Molecular filtration by ultrathin and highly porous silica nanochannel membranes: permeability and selectivity, Anal. Chem. 88 (2016) 10252-10258.

[39] X. Lin, Q. Yang, F. Yan, B. Zhang, B. Su, Gated molecular transport in highly ordered heterogeneous nanochannel array electrode, ACS Appl. Mater. Interfaces 8 (2016) 33343-33349.

[40] M.B. Serrano, C. Despas, G. Herzog, A. Walcarius, Mesoporous silica thin films for molecular sieving and electrode surface protection against biofouling, Electrochem. Commun. 52 (2015) 34-36.

[41] Z. Teng, G. Zheng, Y. Dou, W. Li, C.Y. Mou, X. Zhang, A.M. Asiri, D. Zhao, Highly ordered mesoporous silica films with perpendicular mesochannels by a simple stober-solution growth approach, Angew. Chem. Int. Ed. 51 (2012) 2173-2177.

[42] F. Yan, Y. He, L. Ding, B. Su, Highly ordered binary assembly of silica mesochannels and surfactant micelles for extraction and electrochemical analysis of trace nitroaromatic explosives and pesticides, Anal. Chem. 87 (2015) 4436-4441.

[43] M. Machida, B. Fotoohi, Y. Amamo, L. Mercier, Cadmium(II) and lead(II) adsorption onto hetero-atom functional mesoporous silica and activated carbon, Appl. Surf. Sci. 258 (2012) 7389-7394.

[44] E.M. Roizenblat, K.Z. Brainina, Electrodissolution of mixed metallic deposits from the surface of a solid inert electrode, Elektrokhimiya 5 (1969) 396-403.

[45] K.Z. Brainina., E. Neiman, Electroanalytical stripping methods, J. Willey & Sons, USA, 1993.

[46] X. Xu, G. Duan, Y. Li, G. Liu, J. Wang, H. Zhang, Z. Dai, W. Cai, Fabrication of gold nanoparticles by laser ablation in liquid and their application for simultaneous electrochemical detection of Cd^{2+}, Pb^{2+}, Cu^{2+}, Hg^{2+}, ACS Appl. Mater. Interfaces 6 (2014) 65-71.

[47] W.J. Li, X.Z. Yao, Z. Guo, J.H. Liu, X.J. Huang, Fe_3O_4 with novel nanoplate-stacked structure: surfactant-free hydrothermal synthesis and application in detection of heavy metal ions, J. Electroanal. Chem. 749 (2015) 75-82.

[48] C.M. Quiroa-Montalván, L.E. Gómez-Pineda, L. Álvarez-Contreras, R. Valdez, N. Arjona, M.T. Oropeza-Guzmán, Ordered mesoporous carbon decorated with magnetite for the fetection of heavy metals by dquare eave snodic stripping voltammetry, J. Electrochem. Soc. 164 (2017) 304-313.

[49] S.M. Choi, D.M. Kim, O.S. Jung, Y.B. Shim, A disposable chronocoulometric sensor for heavy metal ions using a diaminoterthiophene-modified electrode doped with graphene oxide, Anal. Chim. Acta 892 (2015) 77-84.

[50] N. Serrano, A. González-Calabuig, M. del Valle, Crown ether-modified electrodes for the simultaneous stripping voltammetric determination of Cd(II), Pb(II) and Cu(II), Talanta 138 (2015) 130-137.

[51] D. Wang, Y. Ke, D. Guo, H. Guo, J. Chen, W. Weng, Facile fabrication of cauliflower-like MIL-100(Cr) and its simultaneous determination of Cd^{2+}, Pb^{2+}, Cu^{2+} and Hg^{2+} from aqueous solution, Sens. Actuators B 216 (2015) 504-510.

[52] F. Gao, N. Gao, A. Nishitani, H. Tanaka, Rod-like hydroxyapatite and nafion nanocomposite as an electrochemical matrix for simultaneous and sensitive detection of Hg^{2+}, Cu^{2+}, Pb^{2+} and Cd^{2+}, J. Electroanal. Chem. 775 (2016) 212-218.

[53] B. Devadas, M. Sivakumar, S.M. Chen, M. Rajkumar, C.C. Hu, Simultaneous and selective detection of environment hazardous metals in water samples by using flower and christmas tree like cerium hexacyanoferrate modified electrodes, Electroanalysis 27 (2015) 2629-2636.

[54] P. Gnanaprakasam, S.E. Jeena, D. Premnath, T. Selvaraju, Simple and robust green synthesis of AuNPs on reduced graphene oxide for the simultaneous detection of toxic heavy metal ions and bioremediation using bacterium as the scavenger, Electroanalysis 28 (2016) 1885-1893.

[55] M. Saadaoui, I. Fernandez, A. Sanchez, P. Diez, S. Campuzano, N. Raouafi, J.M.

Pingarron, R. Villalonga, Mesoporous silica thin film mechanized with a DNAzyme-based molecular switch for electrochemical biosensing, Electrochem. Commun. 58 (2015) 57-61.

[56] Y. Li, X. Huo, J. Liu, L. Peng, W. Li, X. Xu, Assessment of cadmium exposure for neonates in Guiyu, an electronic waste pollution site of China, Environ. Monit. Assess. 177 (2011) 343-351.

[57] H.J. Binns, C. Campbell, M.J. Brown, C. Centers for Disease, P. Prevention advisory vommittee on childhood lead poisoning, interpreting and managing blood lead levels of less than 10 mg/dL in children and reducing childhood exposure to lead: recommendations of the centers for disease control and prevention advisory committee on childhood lead poisoning prevention, Pediatrics 120 (2007) 1285-1298.

TABLES

Table 1 Simultaneous determination of Pb^{2+}, Cu^{2+} and Cd^{2+} in serum and soil leaching solution (SLS).

Sample		Concentration (μM)			
		Added	Found by GFAAS	Found by VMSF/ITO	Recovery[a] by VMSF/ITO (%)
serum[b]	Pb^{2+}	0	0.18	0.19	-
	Cu^{2+}	0	12.81	12.61	-
SLS[b]	Pb^{2+}	0	0.08	0.06	-
	Cu^{2+}	0	0.22	0.19	-
serum[b]	Pb^{2+}	5.00	5.21	5.27	101.6
	Cu^{2+}	5.00	17.76	17.72	102.2
	Cd^{2+}	5.00	5.08	5.24	104.8
SLS[b]	Pb^{2+}	5.00	5.20	5.11	101.0
	Cu^{2+}	5.00	5.16	5.28	101.8
	Cd^{2+}	5.00	4.69	4.89	97.8

[a]Recovery=(determined $C_{metal\ ion}$ of spiked sample - determined $C_{metal\ ion}$ of non-spiked sample)/added value×100%.

[b]The serum and SLS are diluted 5 and 2 times, respectively. For serum samples, protein-bound Pb^{2+}, Cu^{2+} are released from proteins by adding diluted HNO_3.

FIGURES

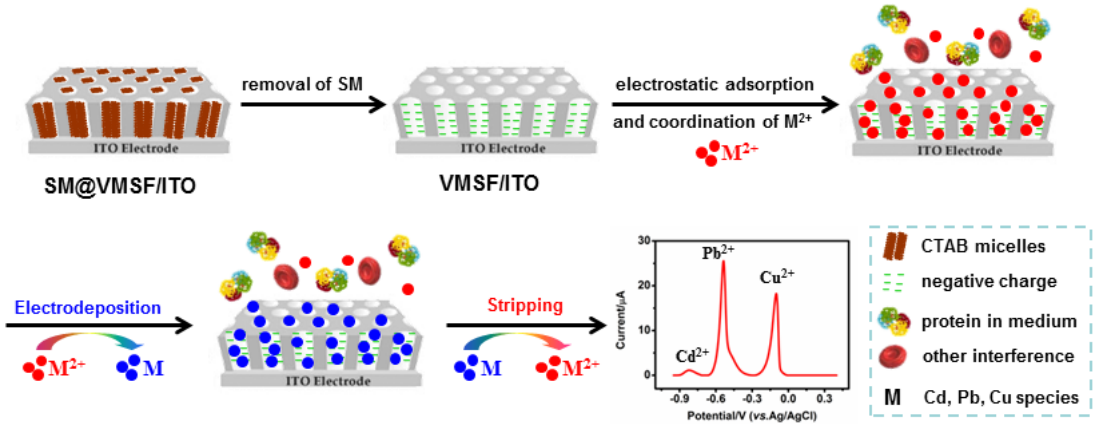

Fig. 1 Schematic illustration of the preparation of VMSF/ITO sensor and its simultaneous detection of Pb^{2+}, Cu^{2+} and Cd^{2+}.

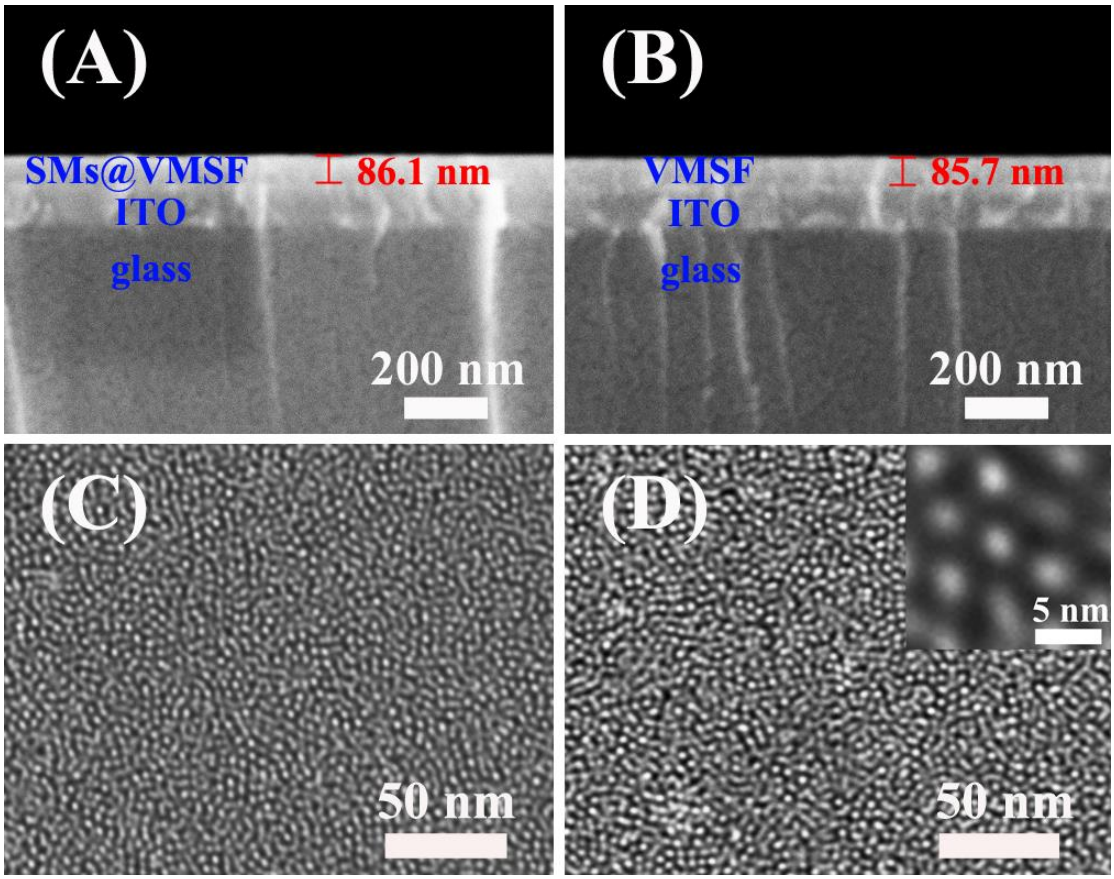

Fig. 2. SEM images of the cross-section of SM@VMSF/ITO (A) and VMSF/ITO (B). High-resolution TEM images (top-view) of SM@VMSF (C) and VMSF (D) scraped from the ITO surface. Inset in (D) shows the magnified view.

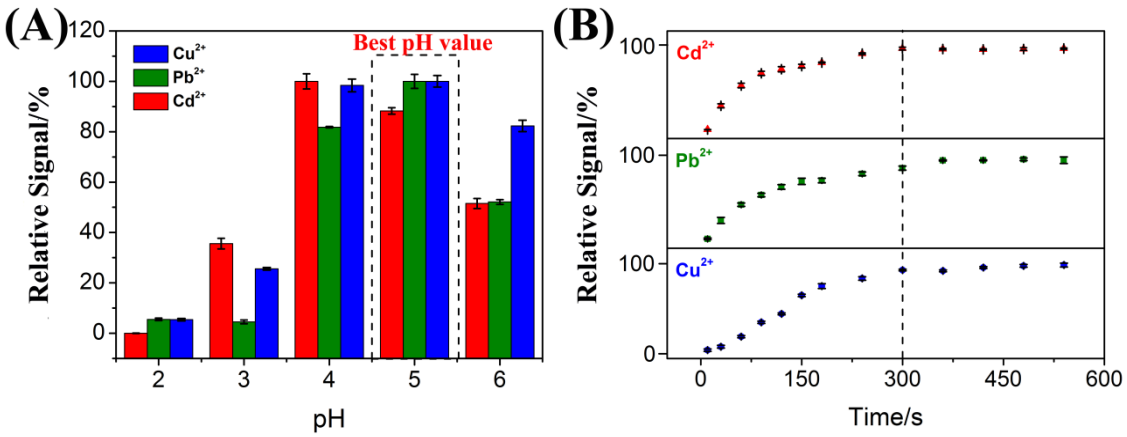

Fig. 3 The effect of pH value (A) and electrodeposition time (B) on the following stripping signal for the detection of Cd^{2+} (red, 5.0 μM), Pb^{2+} (green, 1.0 μM) and Cu^{2+} (blue, 1.0 μM) at VMSF/ITO electrode. The detection signals of the three ions are respectively normalized by using the maximum signal as 100%.

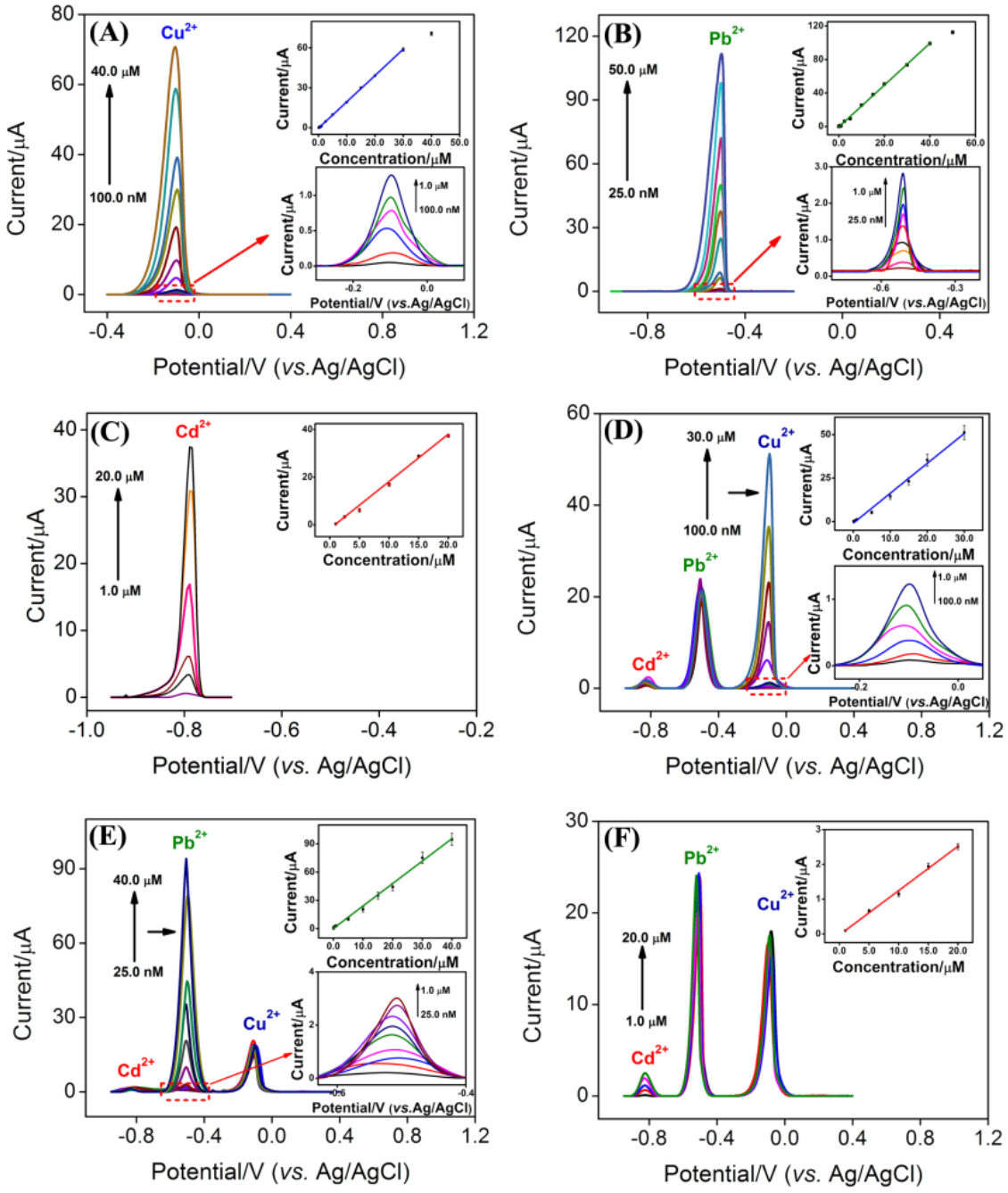

Fig. 4. DPV stripping curves of VMSF/ITO electrode for individual detection of Cu^{2+} (A), Pb^{2+} (B) and Cd^{2+} (C), respectively. DPV stripping curves of VMSF/ITO electrode for detection of Cu^{2+} (D) or Pb^{2+} (E) or Cd^{2+} (F) in presence of fixed concentration of the other two ions (10.0 μM). Upper inset in each figure is the peak current *vs.* ion concentration fitted by a linear line. Lower insets (in A, B, D, E) are the amplified DPV stripping curves at low concentrations.

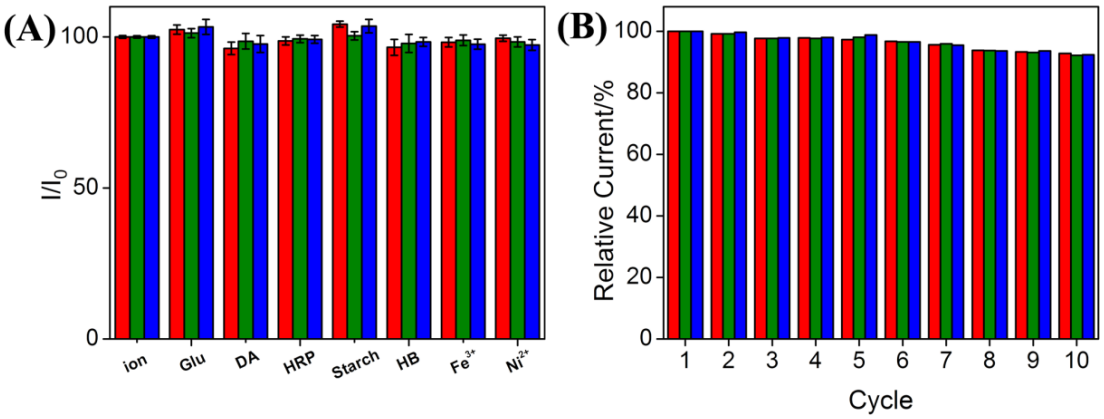

Fig. 5. (A) The current ratio (I/I_0) obtained from VMSF/ITO electrode for detection of Cu^{2+} (blue, 10.0 μM), Pb^{2+} (green, 10.0 μM) and Cd^{2+} (red, 10.0 μM) in absence (I) and presence (I_0) of added interfering substance (600.0 mg/L). (B) The reusability of the VMSF/ITO electrode for detection of Cu^{2+} (blue, 10.0 μM), Pb^{2+} (green, 10.0 μM) and Cd^{2+} (red, 10.0 μM). The initial current in the first detection is set as 100%.

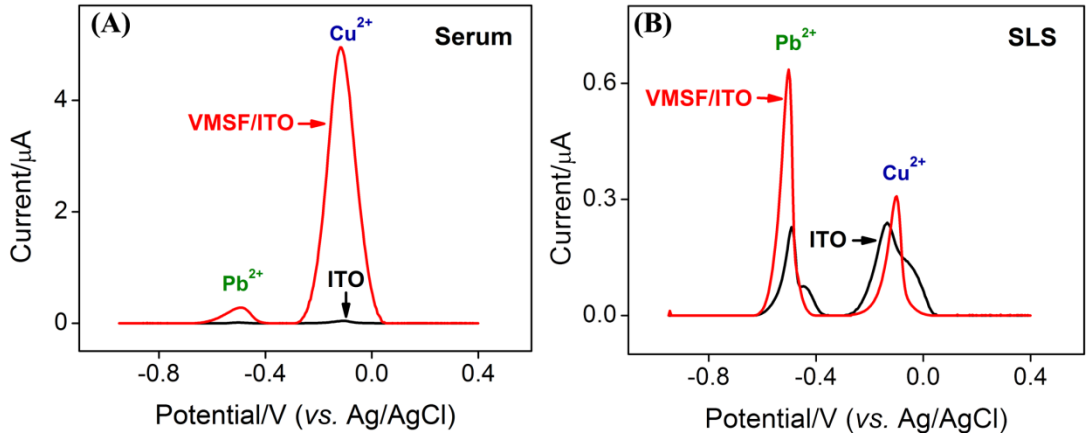

Fig. 6. DPV stripping curves of VMSF/ITO (red line) and ITO (black line) electrode for detection of Cu^{2+} and Pb^{2+} in serum (A) or SLS (B).

SUPPLEMENTARY MATERIALS

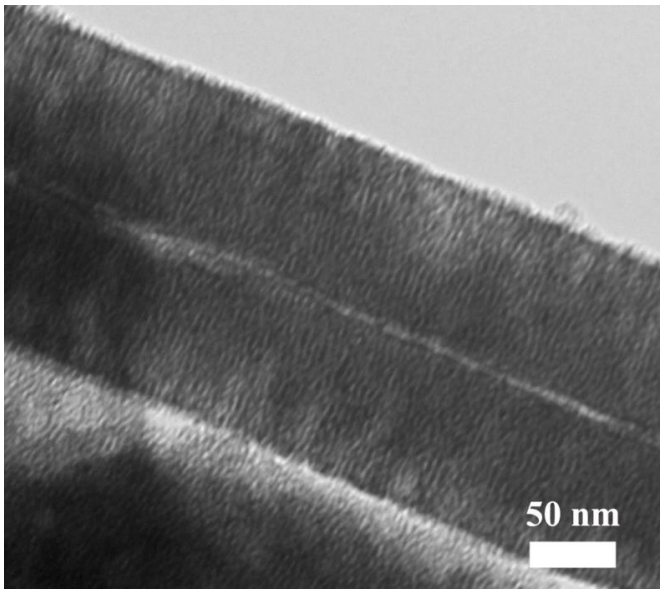

Fig. S1 TEM image of the cross-section of VMSF scraped from the ITO surface.

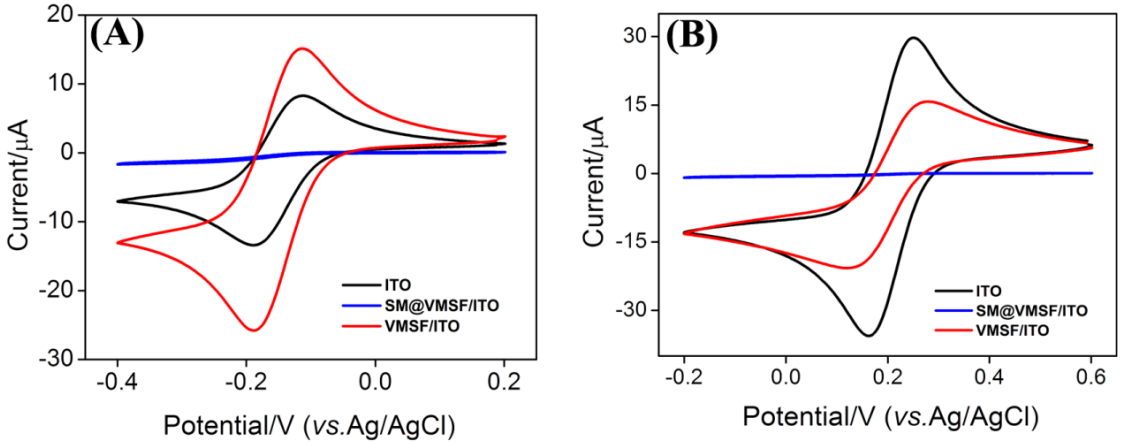

Fig. S2. Cyclic voltammograms of $Ru(NH_3)_6Cl_3$ (A) and $Fe(CN)_6^{3-}$ (B) (both 0.5 mM in 0.05 M KHP, pH 4.0) from SM@VMSF/ITO, VMSF/ITO and ITO electrode.

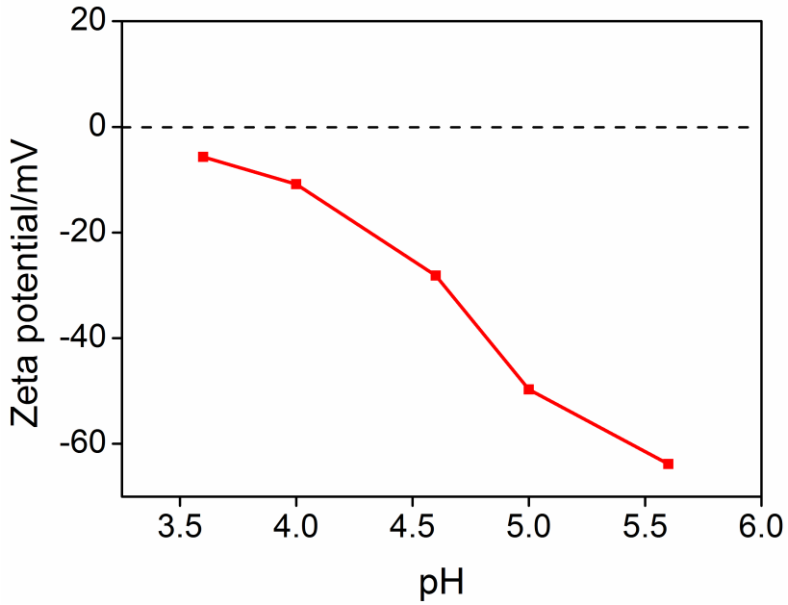

Fig. S3 Zeta potential of VMSF/ITO electrode at different pH value.

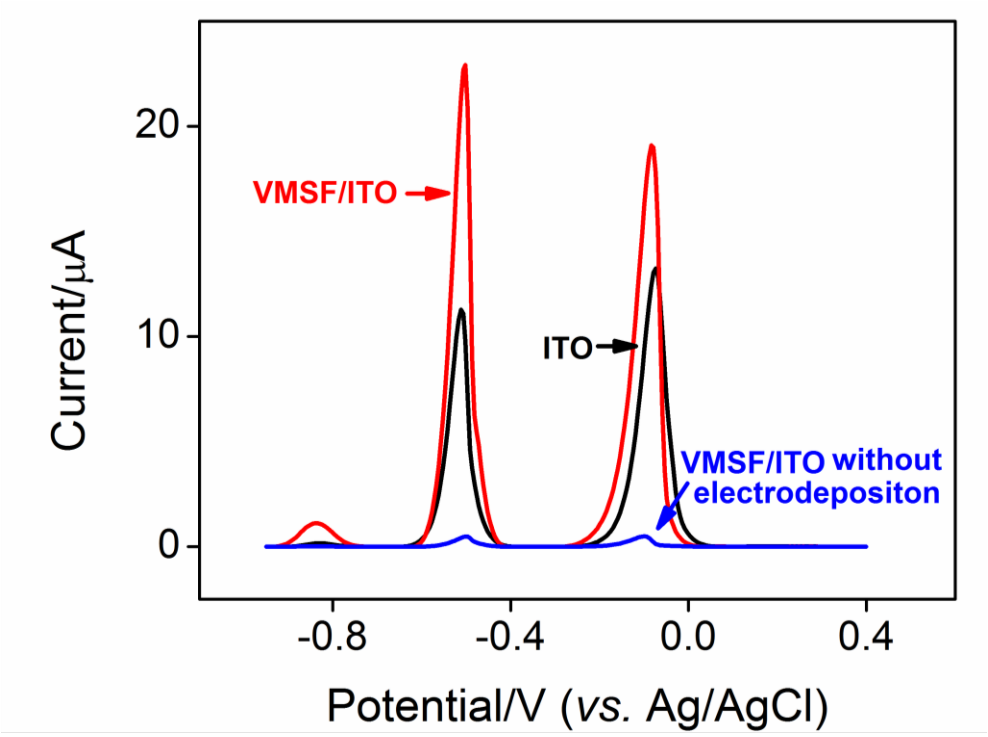

Fig. S4. DPV stripping curves of VMSF/ITO (red line) and ITO (black line) electrode for detection of Cu^{2+}, Pb^{2+} and Cd^{2+}. Blue line is DPV stripping curve of VMSF/ITO electrode for detection of three ions without electrodeposition prior to stripping.

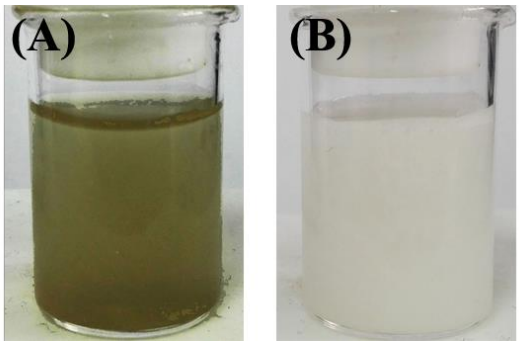

Fig. S5 Digital images of the detected soil leaching solution (A) and serum (B) samples

Table S1 Comparison between electrochemical detection of Cu^{2+}, Pb^{2+} and Cd^{2+} using different modified electrode.

Electrode materials	***Method***	***detection range (μM)***			***LOD (nM)***			*Ref.*
		Cd^{2+}	***Pb^{2+}***	***Cu^{2+}***	***Cd^{2+}***	***Pb^{2+}***	***Cu^{2+}***	
-NH_2 modified VMSF	DPV	-	-	0.01-0.1	-	-	3	33
AuNPs modified GCE	DPV	0.3-1.4	0.3-1.4	0.3-1.4	300	300	300	46
Nanoplate-stacked Fe_3O_4 modified GCE	SWV[a]	0.1-2	0.04-4.2	0.1-1.5	213	59.5	221	47
OMC-OXI-Fe modified graphite	SWV[a]	0.05-4.0	0.02-3.6	0.08-7.0	1650	511	173	48
GO/DTT/Nafion-modified SPCE	SWV[a]	0.009-22	0.005-12	0.002-39	63	9.1	6.3	49
CB-18-crown-6 modified graphite	DPV	0.07-2.0	0.02-0.9	0.08-2.8	21.4	7.2	23.4	50
MIL-100(Cr) modified GCE	DPV	1-10	1-10	1-10	44	48	11	51
Nafion-hydroxyapatite modified GCE	DPV	0.1-10	0.1-10.0	0.1-10.0	35	49	21	52
CeHCF modified GCE	LSV[b]	10-1000	10-1000	10-1000	89.3	9.7	781.2	53
rGO@AuNPs modified GCE	SWV[a]	1-12	1-12	1-12	31.8	12.7	27.4	54
DNAzyme-functionalized VMSF/Au	SWV[a]	-	-	4.8-70.3	-	-	3900	55
VMSF/ITO	DPV	1.0-20.0	0.025-40.0	0.1-30.0	230	2.6	32	This work

[a]SWV is square wave voltammetry.
[b]LSV is linear sweep voltammetry.